Journal of Oncology Research and Therapy
Müller AA, et al. Oncol Res Ther 9: 10234.
www.doi.org/10.29011/2574-710X.10234
www.gavinpublishers.com

OPEN ACCESS

GAVIN PUBLISHERS

Research Article

Targeting DNA Repair Pathways in Orthotopic Glioblastoma Xenoplants

Müller AA[1,2], Kim E[2], Sprang B[2], Schmitt M[1], Vukov Z[1], Mudersbach J[1], Schäfer S[1], Hofmann TG[1*], Nikolova T[1*]

[1]Institute of Toxicology, University Medical Center of the Johannes Gutenberg University Mainz, Obere Zahlbacher Str. 67, Mainz 55131, Germany

[2]Laboratory for Experimental Neurooncology, Clinic for Neurosurgery, Johannes Gutenberg University Medical Centre, Langenbeckstrasse 1, Mainz 55131, Germany

***Corresponding author:** Hofmann TG & Nikolova T, Institute of Toxicology, University Medical Center of the Johannes Gutenberg University Mainz, Obere Zahlbacher Str. 67, Mainz 55131, Germany.

Citation: Müller AA, Kim E, Sprang B, Schmitt M, Vukov Z, et al. (2024) Targeting DNA Repair Pathways in Orthotopic Glioblastoma Xenoplants. J Oncol Res Ther 9: 10234. DOI: 10.29011/2574-710X.10234.

Received Date: 04 July, 2024; **Accepted Date:** 11 July, 2024; **Published Date:** 15 July, 2024

Abstract

Glioblastoma (GBM) is a highly aggressive brain tumor in adults and is notorious for resistance to treatments. Chemotherapy is largely based on alkylating agents that induce lethal secondary DNA double-strand breaks (DSB). Therefore, modulation of DNA DSB-repair pathways that are involved in the innate or acquired tumor resistance, is frequently under consideration for improved chemotherapy. In the present study, we used a RAD51 inhibitor to modulate the DSB repair pathway homologous recombination (HR) and a PARPi to abolish the PARP-dependent non-homologous end-joining (NHEJ) as a backup DSB-repair mechanism in human glioblastoma cells with functional p53 and PTEN. In cell culture, synthetic lethality-like effects of combined treatment with PARPi and RAD51i were observed as well as increased sensitivity to temozolomide when combined with RAD51i or PARPi. In vivo in the orthotopic model, combination of PARPi and RAD51i significantly increased mouse median survival and reduced the tumorigenic potential of cancer xenoplants. Improved survival correlated with increased DNA damage and apoptotic cell numbers, as well as reduced numbers of proliferating cells in tumor brain sections of mice treated with PARPi and RAD51i. Our results suggest that combining RAD51i with PARPi might be beneficial for glioblastoma treatment and suggests RAD51 inhibition as novel strategy in glioma treatment.

Keywords: Glioblastoma; DNA Repair; DNA Double-Strand Break (DSB); DNA Repair Inhibitor; Mouse Orthotopic Model.

Introduction

Glioblastoma multiforme (GBM) is the most aggressive primary brain tumor in adults [1]. GBM is notorious for the high degree of intrinsic and acquired resistance to current standard of care which involves surgical resection followed by radiotherapy with concurrent or subsequent mono- or combined chemotherapy (for review [1-7]). The poor efficacy of standard therapies necessitates intense research to identify novel molecular targets and define more effective therapeutic approaches [8].

Selected methylating or chloro-ethylating agents are used for glioblastoma chemotherapy. Their mode of action is based on modifications of DNA bases (TMZ, procarbazine), or interstrand cross-link formation (lomustine, nimustine) that lead downstream to secondary cytotoxic DSB (for review [5, 9]). Among the potential therapeutic strategies, modulation of the DNA repair pathways that are involved in the innate or acquired tumor resistance, is frequently under consideration. In human cells, there are two main mechanisms for DSB repair: Homologous Recombination (HR) which is error-free and the error-prone Non-Homologous End Joining (NHEJ) pathway. HR is the most important repair pathway for chemically-induced, replication-dependent DSB [10-12]. Therefore, HR is an important target to overcome tumor resistance

to DNA alkylating drugs [13, 14]. In the absence of HR, unrepaired DSB become substrates for PARP [poly(ADP-ribose) polymerase-1] -dependent NHEJ as a back-up mechanism [15]. Actually, PARP plays a role in numerous pathways involved in repair of DNA single-strand and DSB induced by alkylating drugs (for a review [16]). It is well established that cells with functional defects of key HR factors, the so-called BRCAness [17] or HRDness are hypersensitive to PARPi [18, 19]. This mechanism established the clinically interesting principle of synthetic lethality [20]. Recently, it has been suggested that BRCAness in GBM is associated with mutations / deletions in IDH1/2, EGFR, PTEN, MYC proto/oncogene and ERß which are to be considered as biomarkers for responsiveness to PARPi therapy [21]. Among the pointed BRCAness biomarkers, the tumor suppressor PTEN (phosphatase and tensin homolog) is a key regulator of the phosphatidylinositol 3-OH kinase and is known to be frequently mutated or aberrant in GBM [9, 22]. Several studies report radio-sensitization of glioblastoma stem-like cells after PARPi treatment [23, 24], others show modulating effects of PARPi on TMZ response in xenograft models [25, 26]. Based on such findings, several phase I-III clinical trials were approved to treat glioblastoma patients with TMZ in combination with different PARPi [for review [16]]. Key HR proteins like RAD51 can also be targeted by small molecule inhibitors [27, 28] to induce BRCAness and to modulate the responsiveness of GBM cells to standard chemotherapy. For example, we have previously demonstrated that a combination with a RAD51 inhibitor (RAD51i), reduced significantly the growth of subcutaneous glioma xenoplants treated with the chloronitrosourea lomustine [13].

In the present study we used the p53- and PTEN-wild-type (wt) LN229 glioblastoma cell line to determine the sensitivity to the PARPi pamiparib and Rad51i RI-1, applied either as single or combined treatments. Furthermore, we used an orthotopic GBM mouse model [29, 30] to test a combined therapy scheme with a PARPi and a RAD51i for a synthetic lethality-like response in vivo. For our study we selected pamiparib, since at least one biochemical study has demonstrated that this PARPi penetrates through intact blood–brain barrier of GBM patients and can achieve pharmacologically active drug concentrations in the tumor areas [31]. We compared this therapeutic approach to the combination of TMZ with PARPi.

Materials and Methods

Cell Culture and Treatments

The human glioblastoma cell line LN229 was used (see Table S1 Key Resources). All used drugs are listed in Table S1. For the colony formation assay, TMZ was diluted in DMSO at a concentration of 10 mmol/L and stored at -80°C. Upon requirement, aliquots were thawed and added to the cell culture medium or additionally diluted in medium to give a final concentration of 2.5 µmol/L. RAD51i RI-1 was diluted in DMSO to concentration of 25 mmol/L, PARPi pamiparib was diluted also in DMSO to concentration of 5 mmol/L and stored at -80°C. For animal experiments, concentrated solutions of TMZ, RAD51i and PARPi were prepared in DMSO to final concentrations of 10 g/L, 40 g/L and 15 g/L, respectively, and stored at -80°C until required.

Clonogenic Survival Assay

Cells growing in the log phase were used to test colony formation as described [13, 32]. Briefly, cells (n = 400) were seeded in duplicate in cell culture dishes. They were allowed to attach, exposed to 2.5 µmol/L TMZ for 2 hours, and then the medium was changed with or without continuous inhibitor treatment (inhibitor concentrations shown in Fig.2). After 10-day incubation, formed colonies were fixed with 70% ethanol for 10 minutes, stained in crystal violet solution (1 g/L dH2O) for 10 minutes and colonies containing at least 40 cells were counted and presented graphically as a percentage of untreated cells (control). All clonogenic assays were repeated at least 3 times. Statistical significance was evaluated by the two-sided paired t-test in MS Excel.

REAGENT or RESOURCE	SOURCE	IDENTIFIER
Antibodies		
Mouse anti-beta-actin	Santa Cruz Biotechnology	sc-47778
Rabbit anti-Ki67	Abcam	ab16667
Mouse anti-PCNA	Santa Cruz Biotechnology	sc-56
Mouse anti-nestin	R&D	MAB1259
Rabbit anti-nestin	Abcam	ab176571
Rabbit anti-H2AX (Ser139)	Cell Signaling Technology	#9718
Mouse anti-PAR (clone 10H)	A gift by A. Burkle (Fahrer et al., 2009) *	
Donkey anti-Mouse IRDye 800CW	LI-COR Biosciences	925-32212
Donkey anti-Rabbit IRDye 800CW	LI-COR Biosciences	925-32213
Donkey anti-Mouse IRDye 680RD	LI-COR Biosciences	925-68072
Donkey anti-Rabbit IRDye 680RD	LI-COR Biosciences	925-68073
Goat anti-Mouse Cy3-conjugated	Jackson ImmunoResearch Europe	115-166-006
Goat anti-Mouse Alexa488-conj.	Jackson ImmunoResearch Europe	115-546-072
Goat anti-Rabbit Cy3-conjugated	Jackson ImmunoResearch Europe	111-166-045
Goat anti-Rabbit Alexa488-conj.	Jackson ImmunoResearch Europe	111-546-144
Cell lines		
LN-229	ATCC	CRL-2611™
Experimental models: Organisms/strains		
NMRI nude mice	Charles River Europe	NMRI-Fox-1nu/nu
Chemicals, culture media, plasmids and kits		
Advanced DMEM	Thermo Fisher Scientific	12491-023
Temozolomide	Merck (Sigma-Aldrich)	T2577-100MG
Pamiparib (BGB-290)	Selleckchem	S8592
RI-1 (RAD51 inhibitor 1)	Selleckchem	S8077
Captisol (SBE-ß-CD)	Hycultec GmbH	HY-17031
InSitu Cell Death Detection Kit	Sigma-Aldrich (Roche)	11684795910
Streptavidin Cy3™	(Merck) Sigma-Aldrich	S6402
Target Retrieval Solution Citrate	Dako	S2369
Fluoromount Mounting medium	Merck (Sigma-Aldrich)	F4680
TO-PRO-3 Iodide	Thermo Fisher Scientific	#T3605
Software		
ImageJ software	http://imagej.nih.gov/ij	Version 1.52a
GraphPad Prism	GraphPad software, Inc.	version 6.01 for Windows
ZEN Blue	Carl Zeiss Microscopy	Version 3.2.0.
LAS software	Leica Microsystems	Version 4.0.0

Table S1: Key Resources Table.

*Fahrer J, Wagner S, Burkle A, Konigsrainer A. Rapamycin inhibits poly(ADP-ribosyl)ation in intact cells. Biochem Biophys Res Commun 2009; 386: p. 232-6.

Animal Experiments

An orthotopic intracranial murine model [30, 33] was used to evaluate the tumorigenic potential of LN229 GBM PTEN-wt cells in immuno-deficient NMRI-Fox-1nu/nu mice (Charles River). Animal experiments were conducted at the Translational Animal Research Center (TARC) of the University Medical Center Mainz with an approval by the State Office of chemical investigations of Rhineland-Palatinate, Mainz, Germany (permission #23 177-07/G19-1-014). Immunodeficient (nude) mice (strain NMRI, six-week old females) were commercially obtained (Charles River Europe) and housed under SPF or GF conditions in type II EU (European Union) cages inhabited by 2 to 5 companions. The mice were maintained at the standard lab diet for nude mice with water ad libitum, by 22±2°C room temperature and a 12-hour light/dark cycle. All animal groups consisted of female mice that were age-matched and free of clinical symptoms. For intracranial implantation, single cell suspensions of LN229 cells were washed twice in PBS and re-suspended at 15000 cells/µL. Cell suspension (3 µL=45000 cells) was injected into the caudato-putamen of the right hemisphere using a stereotactic frame (TSE Systems, Bad Homburg, Germany) with the following coordinates: 1 mm (anteroposterior axis), 3 mm (lateromedial axis), and 2.5 mm (vertical axis), in reference to the bregma. TMZ treatment started 12 days post implantation. Mice (n=9-10 per group) were injected intraperitoneally for the duration of 21 days. For injections, concentrated TMZ solution (10 g/L) was diluted 1:10 in sterile 0.9% NaCl and injected at a dose of 10 mg/kg body weight each other day for 3 weeks [modified after [29]]. The PARPi was diluted as suggested by the manufacturer in 0.9% NaCl supplied with 10%DMSO and 20% captisol, then injected at a dose of 12 mg/kg body weight each other day [modified after [34]], RAD51i was dissolved in 50 µl corn oil and injected once a week [50 mg/kg body weight as described [13]]. Test animals were terminated at the manifestation of neurological symptoms related to the brain tumor or body weight reduction of >20%, otherwise 28 weeks post implantation at the latest as approved by the authorities. Kaplan-Meier curves were generated based on the survival time of each mouse and survival rates of the treatment groups were compared by the log-rank (Mantel-Cox) test using GraphPad Prism software (version 6.01 for Windows).

Immunohistochemistry on paraffin-embedded glioblastoma sections

We followed a previously described procedure [30, 33, 35, 36]. Briefly, the brains of sacrificed mice were fixed in 4% paraformaldehyde in PBS, sectioned in five parts, which were ordered and embedded together in paraffin. Paraffin blocks were further cooled down, sliced at 1 µm thickness and transferred to slides. For immunohistochemistry, brain sections on slides were deparaffinized by pre-heating at 60°C for 30 min and afterwards incubated in xylene (3×5 min), followed by ethanol series (100/100/96/90/80/70%), and finally rinsed in PBS to rehydrate. Further, specimens were incubated in pre-heated citrate buffer in a steamer for 20 min to retrieve the antigens, then allowed to cool down at room temperature for 20 min. Further, sections were rinsed in PBS then, after blocking, incubated overnight at 4°C with primary antibodies (disclosed in Key Resources Table S1). Incubation with secondary antibodies was performed for 2 h at room temperature: goat Alexa488- or Cy3-conjugated anti-rabbit or anti-mouse (1:600; Jackson ImmunoResearch Eu-rope). Nuclei were counter-stained with TO-PRO–3 (1:100) or DAPI and mounted with Fluoromount fluorescence mounting medium. For To-Pro-3 stained slides, images were taken using the 63x oil objective of LSM710 system equipped with ZEN 2009 software. For tumor area measurements, images were taken on DAPI stained slides using laser micro-scope DMIRB (Leica) equipped with LAS software Version 4.0.0. Images were exported and PCNA, Ki67 or γH2AX positive cells were counted using the Cell Counter function of ImageJ software. Treatment groups (n=3-4 animals per group) were compared by unpaired t-test in MS Excel. Tumor area was measured in square µm in ImageJ and statistical evaluation was performed in MS Excel by unpaired t-test.

Immunofluorescence staining of cells grown on coverslips (Figures S1C and S2A) were performed as previously described [11]. Intranuclear γH2AX foci per nucleus were scored using ImageJ software. Cell clones and treatment variants were compared by unpaired t-test in MS Excel.

TUNEL assay on paraffin embedded sections

In order to detect apoptotic cells in the tumor mass, sections were stained with InSitu Cell Death Detection Kit (Roche) according to a modified version of the manufacturer's protocol. Briefly, reaction mixture was prepared containing 15U of the enzyme terminal deoxynucleotidyl transferase (TdT), 1xBuffer TdT, 1 mM dUTP labeled with biotin, then sections were incubated with 100 µl mixture for 60 min at 37°C. After washing with PBS and blocking, samples were further stained for Nestin to recognize glioblastoma cells. The primary anti–Nestin antibody was recognized by an anti-mouse Alexa488-coupled secondary antibody whereas biotin was tracked by Streptavidin conjugated with Cy3 (1:200). Nuclei were counterstained with To-Pro-3. Counting of TUNEL+ cells and statistical evaluation were performed similar to proliferating cells using ImageJ software and MS Excel.

Results

Increased responsiveness of GBM cells to combined DNA repair inhibitor treatment with PARPi and or RAD51i in cellulo

In order to test the sensitivity of LN229 GBM cells to DNA-damaging tumor treatments including RAD51 inhibitior (RAD51i), PARPi and TMZ we aimed to perform colony formation assays. First, we validated the inhibitory activity of the PARPi pamiparib on formation of poly-ADP-ribose (PAR) polymer foci in the cells upon treatment with H2O2. As expected, PARPi efficiently abolished PAR foci formation indicating its functionality in cells (Figure S1).

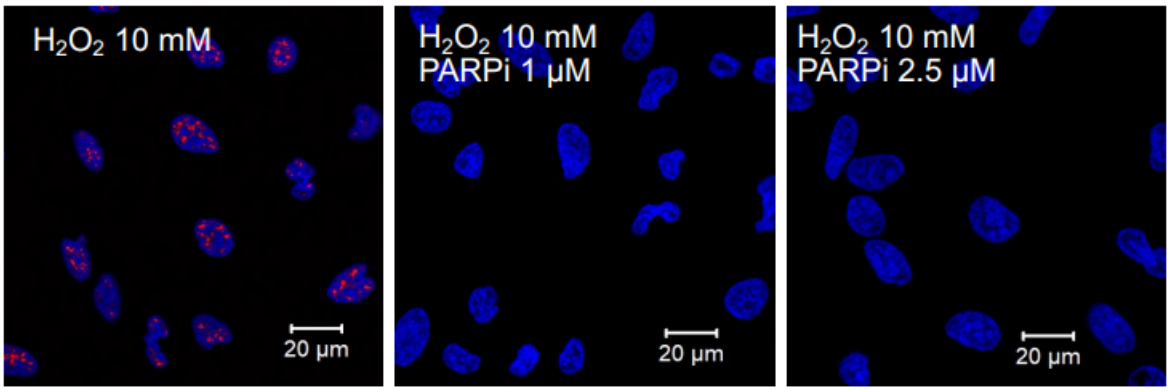

Supplementary Figure S1: PARPi Pamiparib inhibits accumulation or PAR-specific modifications. Immunofluorescence detection of poly-ADP-ribose (PAR)-specific modifications in LN229 cells using a PAR-specific antibody after pretreatment with PARPi for 24 h and treatment with hydrogen peroxide for 5 min

In general, analysis of the colony formation assays indicated that the responsiveness of the GBM cells was relatively low to the used drug concentration for the single treatments, which was intended to be able to determine potential additive or synergistic effects of the drug combinations (Figure 1A, B). Along these lines, significantly higher sensitivity was found to combinatorial drug treatments (Figure 1A, B), which suggests synthetic lethality. In addition, combined treatment of TMZ along with PARPi had a stronger growth inhibitory effect compared to the respective mono treatments. Remarkably, RAD51i, which did not reduce cell survival upon single treatment at the used concentration, significantly potentiated the killing effect of TMZ and of PARPi (Figure 2A, B). Collectively, our results identified drug combinations that show synthetic lethality-like effects and chemosensitization, and identities the combination of RAD51i with TMZ or PARPi as efficient drug combinations.

A

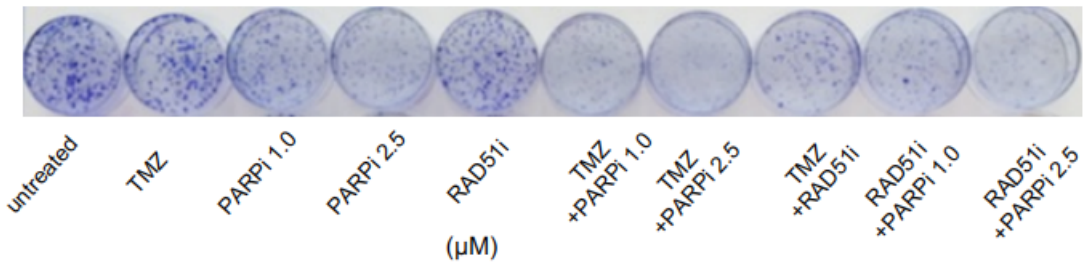

B

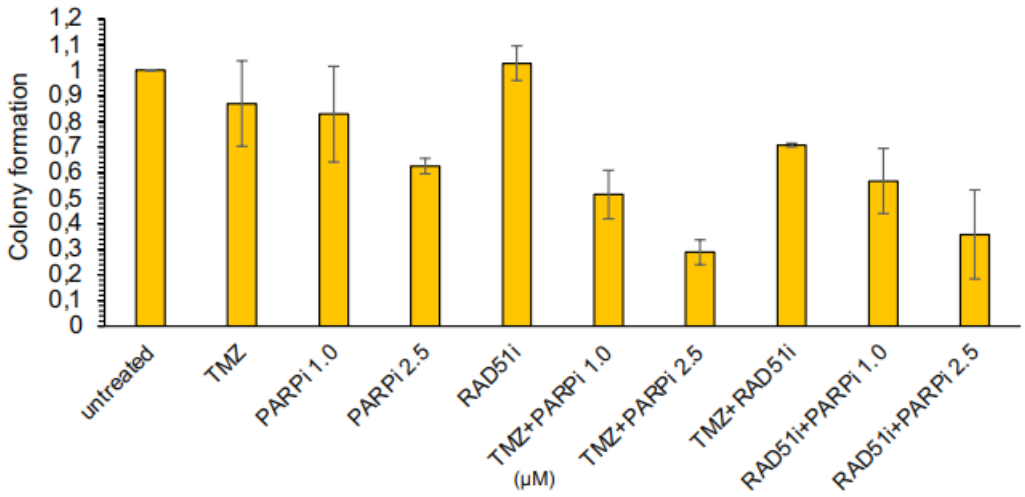

C

p values (two-tailed ttest)	LN229
PARPi 1.0 µM vs. TMZ 2.5 µM+PARPi 1.0 µM	0.01406578
PARPi 2.5 µM vs. TMZ 2.5 µM+PARPi 2.5 µM	0.0092334
RAD51i 5.0 µM vs. TMZ 2.5 µM+RAD51i 5.0 µM	0.01962096
RAD51i 5.0 µM vs. RAD51i 5.0 µM+PARPi 1.0 µM	0.01982373
RAD51i 5.0 µM vs. RAD51i 5.0 µM+PARPi 2.5 µM	0.00935294
PARPi 1.0 µM vs. RAD51i 5.0 µM+PARPi 1.0 µM	0.04442505
PARPi 2.5 µM vs. RAD51i 5.0 µM+PARPi 2.5 µM	0.06528118

Figure 1: Sensitivity of human LN229 glioblastoma cells to TMZ, PARPi, RAD51i and combined treatments in vitro. (A) Representative images of the stained colonies for each treatment variant. Cells (n=400) were seeded in duplicate, after adherence treated for 2 h with TMZ, then inhibitors were added continuously till harvest. Cultures were incubated for 10 days, formed colonies were fixed, stained and counted. (B) Clonogenic survival was determined in the colony formation assay. Each measure point represents the mean of three independent experiments ± standard deviation (SD). (C) p-values of the comparisons of single treatment variants to combined exposure.

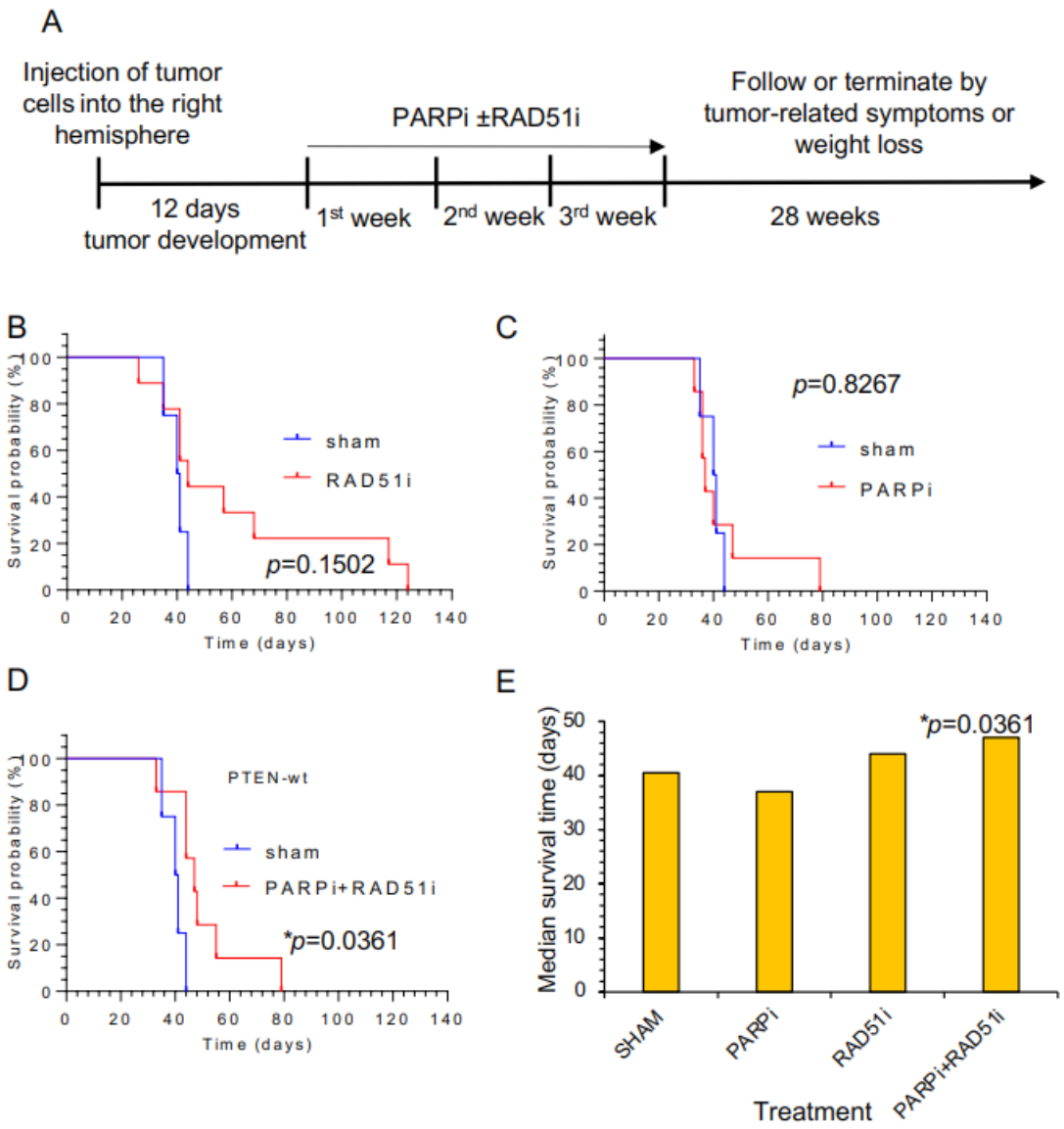

Figure 2: Survival of mice harboring orthotopic GBM after inhibitor treatments. (A) Experimental scheme: Glioblastoma cells (n=40,000) were injected into the brains of NMRI-Fox-1nu/nu mice. Twelve days post implantation, treatment with PARPi (pamiparib), RAD51i (RI-1) or combination of these drugs started. The untreated controls (SHAM) are mice injected with solvent only. Generation of Kaplan-Meier curves and statistical analysis are described in Material and Methods. (B) Survival of SHAM-treated mice vs treated with RAD51i. (C) Survival of SHAM-treated mice vs treated with PARPi. (D) Significantly improved survival of mice treated with RAD51+PARPi (p=0.0361) compared to SHAM-exposed. (E) Median survival times (MST) for each treatment group calculated using GraphPad Prism software.

In vivo analysis of DNA repair inhibitor treatments in mice with orthotopic GBM xenoplants

Our cell culture-based data of the colony formation assays suggested synthetic lethality-like effects in glioblastoma cells after combined exposure to RAD51i and PARPi. Since this drug combination to our best knowledge has not been reported so far for GBM treatment, we aimed to validate our results in vivo using an orthotopic glioblastoma murine model based on intracranial implantation of GBM cells for subsequent tumor growth. In brief, mice were anesthetized and GBM cells were injected into the caudato-putamen of the right hemi-

sphere. Subsequently, mice were housed for 12 days to allow brain tumor growth, then cancer treatments were performed as indicated (Figure 2A). Test animals were sacrificed at the manifestation of neurological symptoms related to the brain tumor growth or body weight reduction over 20%. Survivors were terminated 28 weeks post implantation. Differences in survival rates between the groups were determined on Kaplan-Meier curves using the log-rank (Mantel-Cox) test.

Our results show that, treatment with a combination of PARPi and RAD51i caused significant increase in survival time when compared to the SHAM control group (p=0.03, Figure 2D, 2E). There was also a tendency of prolonged survival following RAD51i treatment alone but the difference did not reach the level of significance (p=0.15, Figure 2B).

Measurements of the tumor areas in the mouse brains confirm the tumor-retarding effects of the combined inhibitor therapy for GBM implants, since in mice treated with both inhibitors it was significantly smaller if compared to those of the SHAM exposed group (p=0.0284, Figure 3B, representative images in Figure 3A). Taken together, our results suggest that also in vivo the combined RAD51i and PARPi treatment is of benefit in a cancer mouse model.

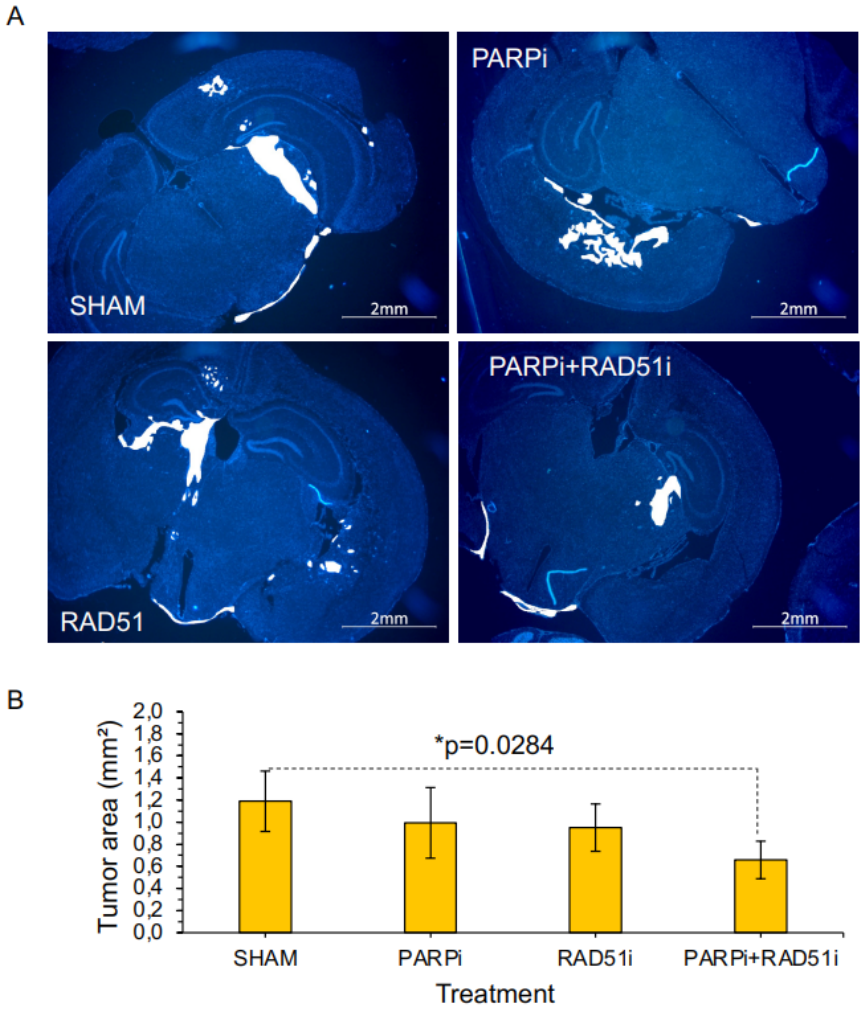

Figure 3: Measurements of the tumor area in brains of mice harboring orthotopic GBM implants. Mouse brains were fixed in 4% paraformaldehyde, sectioned in five parts and paraffin-embedded. 1 µM slices were generated. (A) Representative images of tumor slices from SHAM- or inhibitor treated mice are shown (tumor areas are delineated in white colour). Slide preparation, staining and tumor area measurement are described in Material and Methods. (B) Quantification of tumor area presented in square mm. Statistical evaluation was done using unpaired t-test in MS Excel.

Combined PARPi and Rad51i treatment significantly deminishes GBM proliferation in vivo

Considering that the implanted human glioblastoma cells are the only rapidly dividing cells in the host brain, we used immunofluorescence analysis on brain sections to assess expression of cell proliferation markers. We performed immune-histochemistry double-labeling for the proliferation markers PCNA or Ki67 and the neural stem cell (NSC) marker Nestin, which is known to be also expressed in glioblastoma stem cells [35] and GBM [37]. We counted the PCNA positive cells among the population of Nestin positive glioblastoma cells (representative LSM images in Figure 4A) on brain slices. Of note, the percent of PCNA expressing cells was significantly reduced in the tumors after PARPi or combined PARPi+RAD51i therapy (Figure 4B). Furthermore, we determined the expression of the clinically relevant proliferation marker Ki67 [38-40] (shown in Figure 5A). Cell counts confirmed significantly reduced numbers of Ki67 positive, proliferating tumor cells after combined inhibitor therapy (Figure 5B), and correlated well with the results on PCNA expression. This significant decrease of proliferating tumor in mouse brain slices cells is in accordance with recent evidence that PARPi pamiparib penetrates the blood-brain barrier and is well retained in the tumor tissue [31]. Taken together, these results confirm the tumor growth-retarding effects of the drug combination PARPi +RAD51i.

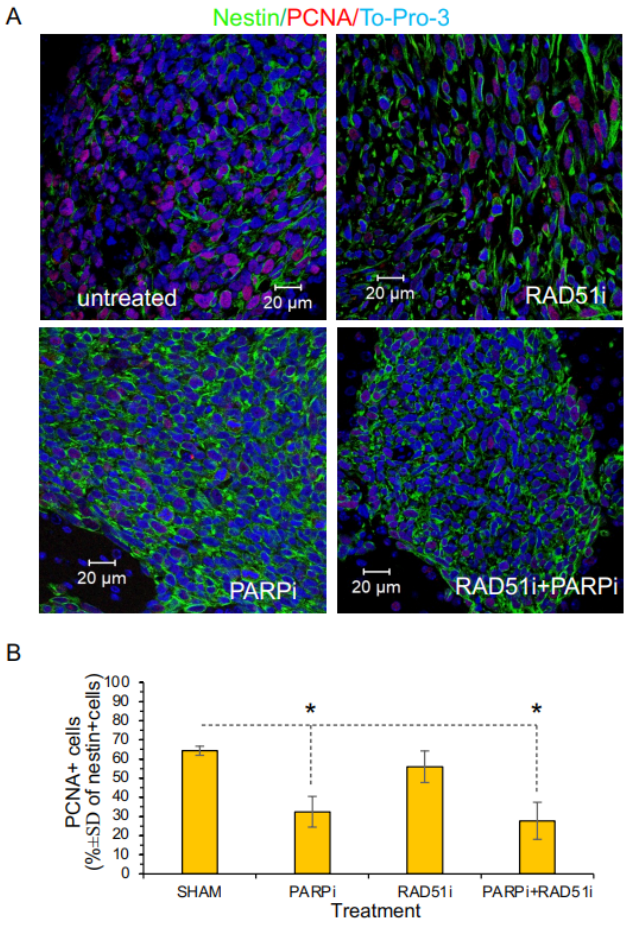

Figure 4: Immunofluorescence-based detection of PCNA in GBM xenoplants in mouse brain tumor sections. (A) Representative images of nestin/PCNA labeling on brain sections from the different treatment groups. Brains of terminated mice (n=3-4) were processed as described in Material and Methods. Sections were incubated with specific primary antibodies against Nestin and PCNA, followed by incubation with secondary antibodies coupled with fluorochromes (red = Cy3, green=Alexa488). Nuclei were counterstained with To-Pro-3. (B) Quantification of PCNA positive cells detected among the population of nestin positive human glio-blastoma cells after SHAM, PARPi, RAD51i or combined inhibitor exposure. Significant decrease of proliferating GBM cells was found after PARPi or combined inhibitor exposure.

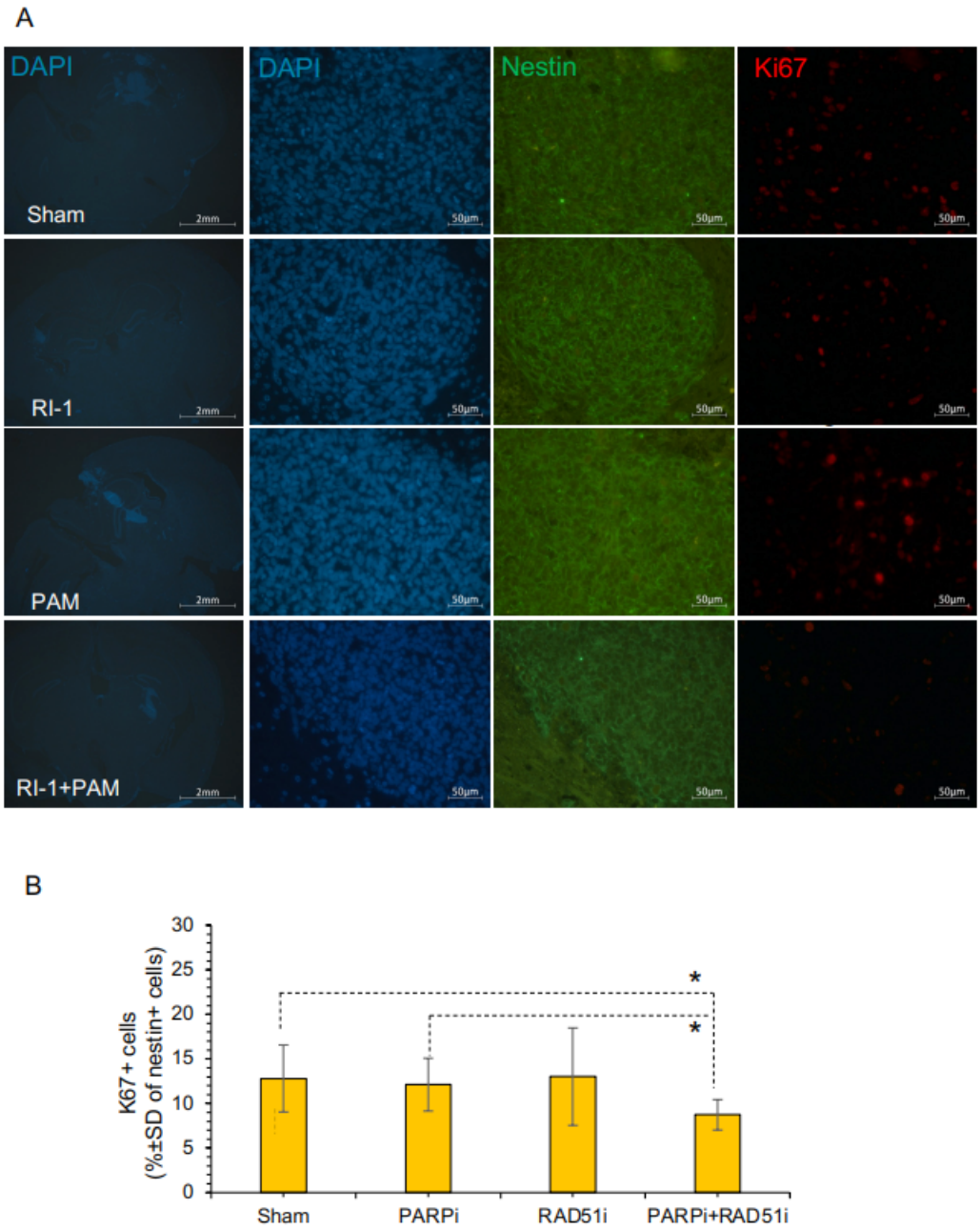

Figure 5: Immunofluorescence-based detection of Ki67 in GBM xenoplants in mouse brain tumor sections. (A) Representative images of Nestin/Ki67 labeling on brain sections from the different treatment groups. Brains were processed as described in Material and Methods. Deparaffinized brain sections were blocked, incubated with specific primary antibodies against NSC marker nestin and proliferation marker Ki67, followed by incubation with secondary antibodies coupled with fluorochromes (red=Alexa555, green=Alexa488) and nuclear counterstaining with DAPI (blue). (B) Quantification of Ki67 positive cells from mice exposed to the vehicle (SHAM), PARPi, RAD51i or inhibitor combination. Statistical evaluation showed significantly less proliferating cells after combined inhibitor exposure compared to SHAM-treated or treated with PARPi alone (*p=0.05).

DNA repair inhibitors lead to increased DSBs in GBM cells in vivo

Further, we expected that the administered DNA repair inhibitors would cause accumulation of DSBs [16] after penetration into the glioblastoma cells. To detect DSBs, we applied a specific antibody against the DSB marker histone 2AXSer139 (γH2AX) (representative images Figure 6A). Despite the quite variable counts of γH2AX foci in the animals from one and the same group, the group treated with the inhibitor combination differed with high significance from SHAM exposed animals (Figure 6B). At least in part, the observed variability might be explained by the fact that the mice were sacrificed at different time points after treatment in accordance with the termination criteria for this pre-clinical animal model.

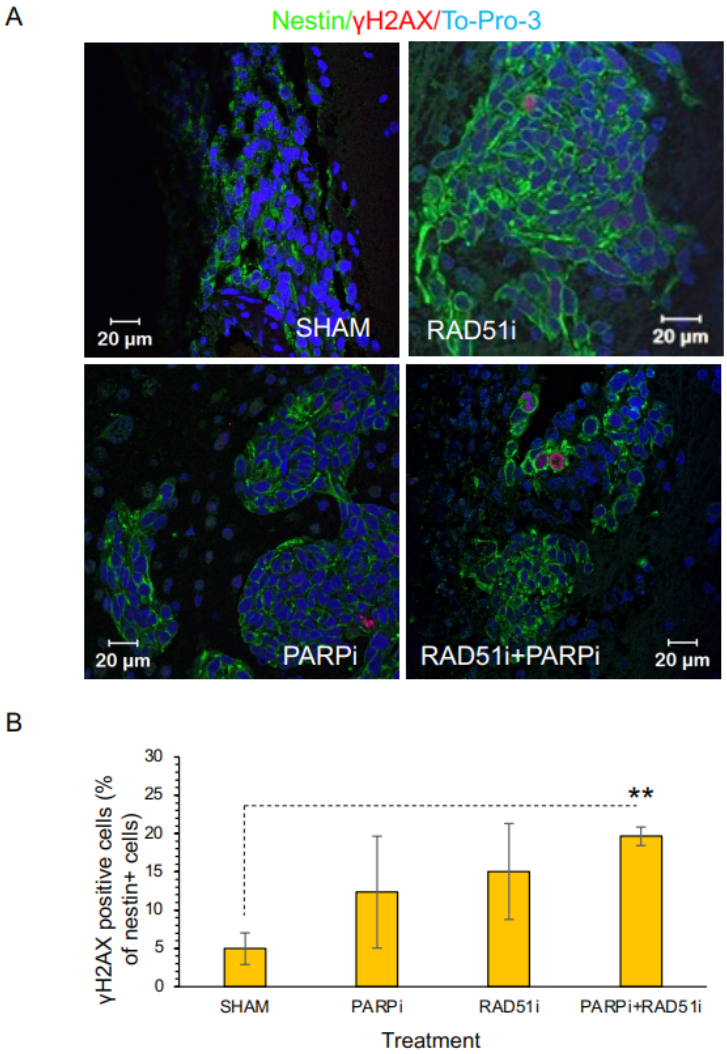

Figure 6: Immunofluorescence-based detection of γH2AX in GBM xenoplants in mouse brain tumor sections. Detection of the DNA damage marker γH2AX on mouse brain sections. (A) Representative images of double staining for Nestin/DNA damage marker γH2AX. Sections were incubated with specific primary antibodies against nestin and γH2AX, followed by incubation with secondary antibodies coupled with fluorochromes (red = Cy3, green=Alexa488). Nuclei were counterstained with To-Pro-3. (B) Quantification of γH2AX positive cells detected among the population of nestin positive human glioblastoma cells after SHAM, PARPi, RAD51i combined inhibitor exposure. γH2AX positive cells were scored using ImageJ software and counts were compared by t-test in MS Excel. Statistical evaluation showed highly significant increase in the number of cells with DNA damage after combined inhibitor exposure compared to SHAM exposure (**p=0.01).

Combined PARPi and Rad51i treatment inceases apoptosis of GBM cells in vivo

Apoptosis is a prominent cell death mechanism activated in response to DSBs induction [41]. Therefore, we investigated whether the observed antitumor effects might be mediated by induction of apoptosis in the orthotopic GBM cancer xenoplants. To this end, we performed TUNEL assays to detect apoptotic cells on brain sections of mice sacrificed at the end of the therapy. To identify the tumor area, we performed co-stainings of Nestin along with TUNEL (Figure 7A). Of note, quantification of the results showed a significant increase of apoptotic TUNEL positive cells after combined RAD51 inhibitor and PARPi treatment (p=0.018) (Figure 7B). A tendency, however, not of significance was also observed after PARPi monotherapy (p=0.0673), whereas RAD51i monotherapy showed no increase in TUNEL positivity (Figure 7B). In association with the decreased tumor areas reported (Figure 3B) and the reduced rate of proliferating cells after these treatments (Figure 4B and Figure 5B), these findings provide an explanation for the (modestly) prolonged median survival after combined inhibitor treatment of mice harboring human glioblastoma-derived tumors. Taken together, our results suggest that combined treatment with RAD51i and PARPi is a promising novel treatment strategy, that might be considered for treatment of GBM in the future.

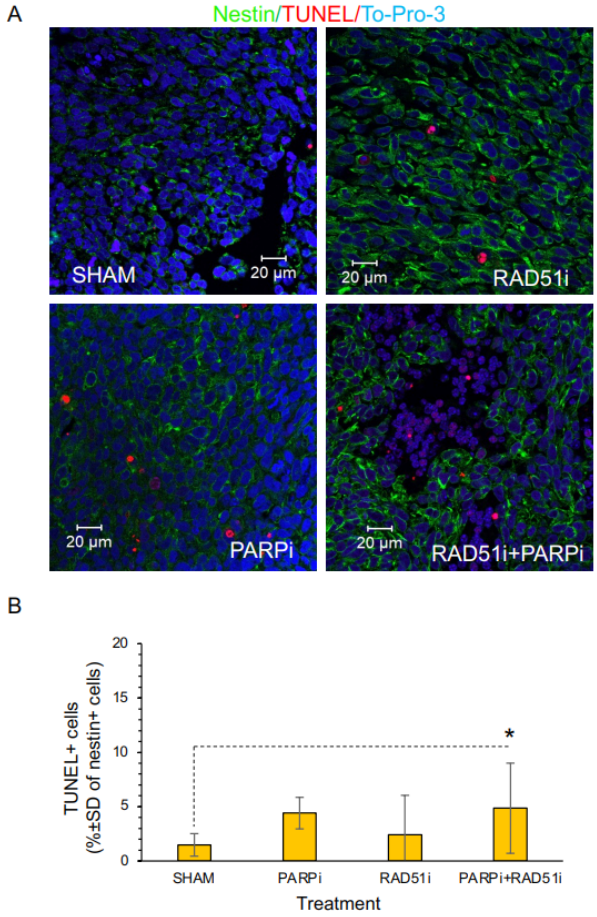

Figure 7: Detection of apoptotic cells by TUNEL assay on mouse brain sections. (A) Representative images of double staining for Nestin/TUNEL. Sections were stained with InSitu Cell Death Detection Kit (Roche), blocked and subsequently stained for nestin. Nestin antibody was recognized by Alexa488-coupled secondary antibody (green), biotin-labeled dUTP (used in the TUNEL reaction) was recognized by Cy3-coupled streptavidin (red) and nuclei were counterstained with To-Pro-3 (blue). (B) Quantification of TUNEL positive cells after SHAM, PARPi, RAD51i or combined inhibitor exposure. Significantly more apoptotic cells were observed after combined inhibitor exposure compared to SHAM exposure (*p=0.05).

Discussion

TMZ is used as a first-choice drug in the chemotherapy of brain tumors and brain metastases of various origins [42-46]. In glioblastoma cells, TMZ induces lethal secondary DSB that are repaired by HR and as a "backup" through PARP-dependent NHEJ [5, 47]. Therapeutic targeting of DNA damage repair pathways using specific small molecules is a widely researched and promising strategy in current cancer therapy. To modulate DSB repair and sensitivity to TMZ in glioblastoma cells, we used a specific small molecule HR inhibitor, the RAD51i RI-1, and a PARPi, namely pamiparib. Our cell culture-based results clearly indicated that combination of PARPi with TMZ or RAD51i efficiently reduced cell growth in glioblastoma cells with functional p53 and PTEN. Interestingly, the in cellulo assays revealed that the combination of TMZ with PARPi was most efficient in reducing colony growth.

Our promising results in cellulo stimulated us to test the most efficient drug combinations in vivo in the intracranial orthotopic GBM mouse model. With the purpose to induce synthetic lethality-like effects in GBM cells, we treated mice harboring human glioblastoma-derived implants with PARPi in combination with RAD51i. Since PARP1/2 DNA repair proteins are known to play a role in the various DSB repair pathways (for a review [48]), additional inhibition of the key HR player RAD51 was expected to block completely the DSB repair and cause lethality in the implanted tumor cells.

We found that treatment with a combination of PARPi and RAD51i led to a significant reduction of tumorigenic potential and increased the survival time of mice harboring human glioblastoma-derived xenografts. Decreased tumorigenic potential was deduced from reduced tumor area as compared to SHAM exposed mice. Additional evidence gave the significantly decreased numbers of PCNA+ and Ki67+ proliferating cells and increased numbers of apoptotic TUNEL+ cells in the immunofluorescence analyses on brain sections.

Interestingly, orthotopic tumors grown from p53 and PTEN proficient implants were highly sensitive to TMZ treatment, which is in accordance with previous observations in a similar intracranial mouse model [29]. Since all mice with GBM survived the observation period after TMZ monotherapy, no beneficial effect of PARPi addition could be established. In general, the present results indicate that in vivo TMZ treatment alone is superior to the DNA repair inhibitor treatments (single or combined for synthetic lethality-like effect) of glioblastoma implants, which is most probably, due to the high induction of DSBs by TMZ [14]. In summary, our study suggests that the combination of RAD51i with PARPi should be considered as an interesting novel drug combination for GBM treatment. However, this will require additional research in tumors with p53 and PTEN mutations as a novel therapeutic approach for the treatment of GBM patients with resistance to classical chemotherapy.

Author Contributions: A.M.– animal experiments, tissue slide preparation, immunohistochem-istry analysis, data analysis, E.K.- animal experiments, data discussion and contribution to man-uscript writing, B.S.- tissue slide preparation, immunohistochemistry analysis, M.S., Z.V. colony formation analysis, T.G.H.- data discussion, interpretation and contribution to manuscript writing; T.N. –design and supervision of all experiments, animal experiments, immunohistochemistry analysis, manuscript preparation.

Funding: The study was supported by DFG (German Research Foundation) grant Ni1319/3 to TN, and the Internal University Research Funding of JGU Mainz to TN (2021-2022).

Acknowledgement: We thank Birgit Rasenberger for excellent technical assistance and Nancy Berte for help with FACS sorting.

Conflicts of Interest: The authors declare no potential conflicts of interest regarding the re-search, authorship or publication of this article.

References

1. Patel MA, Kim JE, Ruzevick J, Li G, Lim M (2014) The future of glioblastoma therapy: synergism of standard of care and immunotherapy. Cancers (Basel) 6:1953-85.
2. Alexander BM, Ba S, Berger MS, Berry DA, Cavenee WK, et al. (2018) Adaptive Global Innovative Learning Environment for Glioblastoma: GBM AGILE. Clin Cancer Res 24:737-743.
3. Alexander BM, Cloughesy TF (2017) Adult Glioblastoma. J Clin Oncol 35:2402-2409.
4. Fernandes C, Costa A, Osório L, Lago RC, Linhares P, et al. (2017) Current Standards of Care in Glioblastoma Therapy. in Glioblastoma, S. 2017: Brisbane (AU).
5. Nikolova T, Roos WP, Krämer OH, Strik HM, Kaina B (2017) Chloroethylating nitrosoureas in cancer therapy: DNA damage, repair and cell death signaling. Biochim Biophys Acta Rev Cancer 1868:29-39.
6. Weller M, Rhun EL (2020) How did lomustine become standard of care in recurrent glioblastoma? Cancer Treat Rev 87:102029.
7. Wirsching HG, Galanis E, Weller M (2016) Glioblastoma. Handb Clin Neurol 134:381-97.
8. Yalamarty SSK, Filipczak N, Li X, Subhan MA, Parveen F, et al. (2023) Mechanisms of Resistance and Current Treatment Options for Glioblastoma Multiforme (GBM). Cancers (Basel) 15:2116.
9. Vilar JB, Christmann M, Tomicic MT (2022) Alterations in Molecular Pro?les Affecting Glioblastoma Resistance to Radiochemotherapy: Where Does the Good Go? . Cancers 14:2416.
10. Nikolova T, Ensminger M, Löbrich M, Kaina B (2010) Homologous recombination protects mammalian cells from replication-associated DNA double-strand breaks arising in response to methyl methanesulfonate. DNA Repair (Amst) 9:1050-63.

11. Nikolova T, Hennekes F, Bhatti A, Kaina B (2012) Chloroethylnitrosourea-induced cell death and genotoxicity: cell cycle dependence and the role of DNA double-strand breaks, HR and NHEJ. Cell Cycle 11:2606-19.

12. Roos WP, Nikolova T, Quiros S, Naumann SC, Kiedron O, et al. (2009) Brca2/Xrcc2 dependent HR, but not NHEJ, is required for protection against O(6)-methylguanine triggered apoptosis, DSBs and chromosomal aberrations by a process leading to SCEs. DNA Repair (Amst) 8:72-86.

13. Berte N, Piée-Staffa A, Piecha N, Wang M, Borgmann K, et al. (2016) Targeting homologous recombination by pharmacological inhibitors enhances the killing response of glioblastoma cells treated with alkylating drugs. Mol Cancer Ther 15:2665-2678.

14. Quiros S, Roos WP, Kaina B (2011) Rad51 and BRCA2--New molecular targets for sensitizing glioma cells to alkylating anticancer drugs. PLoS One 6:e27183.

15. Bryant HE, Petermann E, Schultz N, Jemth AS, Loseva O, et al. (2009) PARP is activated at stalled forks to mediate Mre11-dependent replication restart and recombination. EMBO J 28:2601-15.

16. Gupta SK, Smith EJ, Mladek AC, Tian S, Decker PA, et al. (2018) PARP Inhibitors for Sensitization of Alkylation Chemotherapy in Glioblastoma: Impact of Blood-Brain Barrier and Molecular Heterogeneity. Front Oncol 8:670.

17. Byrum AK, Vindigni A, Mosammaparast N (2019) Defining and Modulating 'BRCAness'. Trends Cell Biol 29:740-751.

18. Bryant HE, Schultz N, Thomas HD, Parker KM, Flower D, et al. (2005) Specific killing of BRCA2-deficient tumours with inhibitors of poly(ADP-ribose) polymerase. Nature 434:913-7.

19. Farmer H, McCabe N, Lord CJ, Tutt ANJ, Johnson DA, et al. (2005) Targeting the DNA repair defect in BRCA mutant cells as a therapeutic strategy. Nature 434:917-21.

20. Hartwell LH, Szankasi P, Roberts CJ, Murray AW, Friend SH (1997) Integrating genetic approaches into the discovery of anticancer drugs. Science 278:1064-8.

21. Xavier MA, Resende F, Titze-de-Almeida R, Cornelissen B (2021) BRCAness as a Biomarker of Susceptibility to PARP Inhibitors in Glioblastoma Multiforme. Biomolecules 11:1188.

22. Benitez JA, Ma J, Antonio MD, Boyer A, Camargo MF, et al. (2017) PTEN regulates glioblastoma oncogenesis through chromatin-associated complexes of DAXX and histone H3.3. Nat Commun 8:15223.

23. Carruthers RD, Ahmed SU, Ramachandran S, Strathdee K, Kurian KM, et al. (2018) Replication Stress Drives Constitutive Activation of the DNA Damage Response and Radioresistance in Glioblastoma Stem-like Cells. Cancer Res 78:5060-5071.

24. Lesueur P, Chevalier F, El-Habr EA, Junier MP, Chneiweiss H, et al. (2018) Radiosensitization Effect of Talazoparib, a Parp Inhibitor, on Glioblastoma Stem Cells Exposed to Low and High Linear Energy Transfer Radiation. Sci Rep 8:3664.

25. Gupta SK, Kizilbash SH, Carlson BL, Mladek AC, Boakye-Agyeman F, et al. (2016) Delineation of MGMT Hypermethylation as a Biomarker for Veliparib-Mediated Temozolomide-Sensitizing Therapy of Glioblastoma. J Natl Cancer Inst 108:djv369.

26. Lemasson B, Wang H, Galban S, Li Y, Zhu Y, et al. (2016) Evaluation of Concurrent Radiation, Temozolomide and ABT-888 Treatment Followed by Maintenance Therapy with Temozolomide and ABT-888 in a Genetically Engineered Glioblastoma Mouse Model. Neoplasia 18: 82-9.

27. Dupre A, Boyer-Chatenet L, Sattler RM, Modi AP, Lee JH, et al. (2008) A forward chemical genetic screen reveals an inhibitor of the Mre11-Rad50-Nbs1 complex. Nat Chem Biol 4:119-25.

28. Huang F, Motlekar NA, Burgwin CM, Napper AD, Diamond SL, et al. (2011) Identification of specific inhibitors of human RAD51 recombinase using high-throughput screening. ACS Chem Biol 6:628-35.

29. Berte N, Lokan S, Eich M, Kim E, Kaina B (2016) Artesunate enhances the therapeutic response of glioma cells to temozolomide by inhibition of homologous recombination and senescence. Oncotarget 7:67235-67250.

30. Kalasauskas D, Sorokin M, Sprang B, Elmasri A, Viehweg S, et al. (2020) Diversity of Clinically Relevant Outcomes Resulting from Hypofractionated Radiation in Human Glioma Stem Cells Mirrors Distinct Patterns of Transcriptomic Changes. Cancers (Basel) 12:570.

31. Jiang J, Bao X, Yue Y, Schiff D, Bindra R, et al. (2022) Development and validation of a liquid chromatography coupled with tandem mass spectrometry method for determining total and unbound pamiparib in human plasma and brain tumors. Biomed Chromatogr 36:e5478.

32. Hill P, Zellmann F, Vukova T, Marini F, Kolmar S, et al. (2022) Dose response to methylating agents in the gammaH2AX, SCE and colony formation assays: Effect of MGMT and MPG overexpression. Mutat Res Genet Toxicol Environ Mutagen 876-877:503462.

33. Muller A, Weyerhauser P, Berte N, Jonin F, Lyubarskyy B, et al. (2023) Concurrent Activation of Both Survival-Promoting and Death-Inducing Signaling by Chloroquine in Glioblastoma Stem Cells: Implications for Potential Risks and Benefits of Using Chloroquine as Radiosensitizer. Cells 12:1290.

34. Gupta SK, Carlson BL, Schroeder MA, Bakken KK, Tuma AC, et al. (2015) Inhibition of PARP activity by BGB-290 potentiates efficacy of temozolomide in patient derived xenografts of glioblastoma multiforme. Cancer Res 75:3505.

35. Fauss J, Sprang B, Leukel P, Sommer C, Nikolova T, et al. (2021) ALDH1A3 Segregated Expression and Nucleus-Associated Proteasomal Degradation Are Common Traits of Glioblastoma Stem Cells. Biomedicines 10:7.

36. Reich TR, Schwarzenbach C, Vilar JB, Unger S, Muhlhausler F, et al. (2021) Localization matters: nuclear-trapped Survivin sensitizes glioblastoma cells to temozolomide by elevating cellular senescence and impairing homologous recombination. Cell Mol Life Sci 78:5587-5604.

37. Zhang M, Song T, Yang L, Chen R, Wu L, et al. (2008) Nestin and CD133: valuable stem cell-specific markers for determining clinical outcome of glioma patients. J Exp Clin Cancer Res 27: 85.

38. Stark AM, Doukas A, Hugo HH, Mehdorn HM (2010) The expression of mismatch repair proteins MLH1, MSH2 and MSH6 correlates with the Ki67 proliferation index and survival in patients with recurrent glioblastoma. Neurol Res 32:816-20.

39. Nafe R, Herminghaus S, Raab P, Wagner S, Pilatus U, et al. (2003) Correlation between preoperative magnetic resonance spectroscopic data on high grade gliomas and morphology of Ki-67-positive tumor cell nuclei. Anal Quant Cytol Histol 25:131-8.

40. Nafe R, Franz K, Schlote W, Schneider B (2003) Quantitative investigation of nuclear morphology in glioblastomas and its relation to survival time. Clin Neuropathol 22:129-36.

41. Matt S, Hofmann TG (2016) The DNA damage-induced cell death response: a roadmap to kill cancer cells. Cell Mol Life Sci 73:2829-50.

42. Chua J, Nafziger E, Leung D (2019) Evidence-Based Practice: Temozolomide Beyond Glioblastoma. Curr Oncol Rep 21:30.

43. Hotchkiss KM, Sampson JH (2021) Temozolomide treatment outcomes and immunotherapy efficacy in brain tumor. J Neurooncol 151:55-62.

44. Peereboom DM (2005) Chemotherapy in brain metastases. Neurosurgery 57:S54-65; discusssion S1-4.

45. Yang Y, Pu Y, Dai N, Wang D, Xu M (2020) Complete response of radioresistant brain metastases from non-small cell lung cancer with temozolomide: A case report and literature review. Medicine (Baltimore) 99:e23592.

46. Zimmer AS, Steinberg SM, Smart DD, Gilbert MR, Armstrong TS, et al. (2020) Temozolomide in secondary prevention of HER2-positive breast cancer brain metastases. Future Oncol 16:899-909.

47. Nikolova T, Kramer OH (2019) Targeting DNA double-strand break repair for glioblastoma chemotherapy. Science World Journal of cancer Science and Therapy 1:1-4.

48. Faraoni I, Graziani G (2018) Role of BRCA Mutations in Cancer Treatment with Poly(ADP-ribose) Polymerase (PARP) Inhibitors. Cancers (Basel) 10:487.